

Synthesis of Isorecticular Zinc(II)-Phosphonocarboxylate Frameworks and Their Application in the Friedel–Crafts Benzylolation Reaction

Mingli Deng, Yun Ling, Bing Xia, Zhenxia Chen, Yaming Zhou,* Xiaofeng Liu, Bin Yue, and Heyong He*^[a]

Abstract: Three isorecticular zinc(II)-phosphonocarboxylate frameworks, namely $\{[\text{Zn}_3(\text{pbdc})_2] \cdot 2\text{H}_2\text{O}\}_n$ (ZnPC-2), $\{[\text{Zn}_3(\text{pbdc})_2] \cdot \text{Hpd} \cdot \text{H}_3\text{O} \cdot 4\text{H}_2\text{O}\}_n$ (Hpd@ZnPC-2) and $\{[\text{Co}_{1.5}\text{Zn}_{1.5}(\text{pbdc})_2] \cdot 2\text{H}_2\text{O}\}_n$ (CoZnPC-2) (H_4pbdc = 5-phosphonobenzene-1,3-dicarboxylic acid, pd = pyrrolidine), were solvothermally synthesized. ZnPC-2 has a 3D structure based on trinuclear Zn^{II} clusters (Zn_3 -SBU) showing 3D in-

terconnected channels. Hpd@ZnPC-2 contains an isorecticular framework of ZnPC-2 with small channels blocked by Hpd molecules. In CoZnPC-2, Zn^{II} ions in ZnPC-2 are partially substituted

Keywords: heterogeneous catalysis • isorecticular structure • metal–organic frameworks • phosphonate ligands • zinc

by Co^{II} ions. The Friedel–Crafts benzylolation reactions were carried out over these isorecticular porous materials. The catalytic results reveal that ZnPC-2 is an excellent heterogeneous Lewis acid catalyst with a high selectivity (> 90%) towards less bulky *para*-oriented products. The catalytic reaction has been proved to occur inside the pore of ZnPC-2, and the immobilized Zn_3 -SBUs are the active sites.

Introduction

Catalytic alkylation of aromatics is a very important C–C coupling reaction and has been undertaken on a large scale in both petrochemical and chemical industries.^[1–3] The *para*-oriented dialkylated aromatics, such as *para*-diisopropylbenzene, *para*-ethyltoluene, *para*-diethylbenzene, *para*-cymenes and 4-*tert*-butyltoluene, are very important chemical materials. The Friedel–Crafts reaction is a typical catalytic alkylation reaction and generally results the mixture of *para*-, *meta*- and *ortho*-oriented products. Traditionally, strong mineral acids (such as HF and H_2SO_4) and Lewis acids (such as AlCl_3 , FeCl_3 and ZnCl_2) have been used as the catalysts. These traditional catalysts, however, not only cause undesirable economic and environmental problems in separating and handling of the acid waste,^[4–5] but also suffer low selectivity towards the *para* products.^[6] Thus, there is a strong demand to replace these catalysts with green and efficient heterogeneous catalysts. H-form zeolites have been studied as the catalysts in the Friedel–Crafts alkylation reactions,^[7–8] because of their strong acidity and microporosity. However, the small pore size of zeolites limits its application in the al-

kylation of bulky aromatic molecules. Therefore, increasing interests have been focused on the porous metal–organic frameworks (MOFs).

MOFs have attracted tremendous interest during the past decades due to their potential applications in gas storage and/or separation, molecular recognition, ion exchange, drug delivery and so on.^[9–14] Compared with other porous materials, the unique features of MOFs, are their designable structures,^[15–17] adjustable pore sizes (from microspore to mesopore)^[18–24] and controllable host–guest interactions inside the pores (from hydrophobic to hydrophilic, polarity to no polarity).^[25–26] On the other hand, MOFs possess inherent advantages as no additional support is needed for the heterogenization, and the organic microenvironment provided by the framework often allows the metal active sites to behave in a manner reminiscent of enzymes.^[27–29] However, it must be realized that only limited investigations of MOFs have been carried out in heterogeneous catalysis compared with the number of structures discovered and the achievements in gas storage and separation.^[30–33] Recently, the Friedel–Crafts benzylolation reactions using MOFs (such as MOF-*n* and MIL-*n*) as the catalysts have been explored.^[6,34–37] However, this study has been generally focused on the catalytic performance of certain reported MOFs. The use of the approach of isorecticular MOFs as catalysts to explore catalytic active sites, as far as we know, is rarely reported due to the challenges to obtain isorecticular MOFs.^[17,38–40]

The present work aims to synthesize isorecticular frameworks and explore their catalytic reaction and related active sites in the Friedel–Crafts benzylolation reaction. $\{[\text{Zn}_3(\text{pbdc})_2] \cdot 2\text{H}_2\text{O}\}_n$ (ZnPC-2, H_4pbdc = 5-phosphonobenzene-1,3-dicarboxylic acid) is a porous rutile-type framework con-

[a] M. Deng,⁺ Dr. Y. Ling,⁺ B. Xia, Dr. Z. Chen, Dr. Y. Zhou, X. Liu, Dr. B. Yue, Dr. H. He

Department of Chemistry and Shanghai Key Laboratory of Molecular Catalysis and Innovative Materials
Fudan University, 220 Handan Road
Shanghai 200433, (P. R. China)
E-mail: ymzhou@fudan.edu.cn
heyonghe@fudan.edu.cn

[⁺] M. L. Deng and Y. Ling contributed equally to this paper.

Supporting information for this article is available on the WWW under <http://dx.doi.org/10.1002/chem.201101239>.

structured by six-connected $\text{Zn}_3(\text{CO}_2)_4(\text{PO}_3)_2$ secondary building blocks ($\text{Zn}_3\text{-SBU}$) and tritopic 5-phosphonobenzene-1,3-dicarboxylic acid, showing 3D interconnected regular channels (ca. $6 \times 6 \text{ \AA}$ along the c axis, ca. $4 \times 4 \text{ \AA}$ along a and b axes). $\{[\text{Zn}_3(\text{pbdc})_2] \cdot \text{Hpd} \cdot \text{H}_3\text{O} \cdot 4\text{H}_2\text{O}\}_n$ (pd=pyrrolidine, named as Hpd@ZnPC-2) is an isoreticular framework with only 1D channels along the c axis (ca. $5 \times 5 \text{ \AA}$) and $\{[\text{Co}_{1.5}\text{Zn}_{1.5}(\text{pbdc})_2] \cdot 2\text{H}_3\text{O}\}_n$ is a Co^{II} -partially-substituted ZnPC-2 (CoZnPC-2). The catalytic results show that the ZnPC-2 is an efficient heterogeneous acid catalyst for the Friedel-Crafts benzylation reaction with a high selectivity (>90%) to the *para*-oriented product. The catalytic reaction and the active sites of ZnPC-2 have been studied for the first time based on the isoreticular frameworks of Hpd@ZnPC-2 and CoZnPC-2.

Results and Discussion

Synthesis and characterization: Crystalline samples of rutile-type porous ZnPC-2 (Figure 1a) with high yields were prepared according to our previous method^[41] with some modification described in the Experimental Section. ZnPC-2 consists of trimeric zinc-phosphonocarboxylate clusters (Zn_3 -

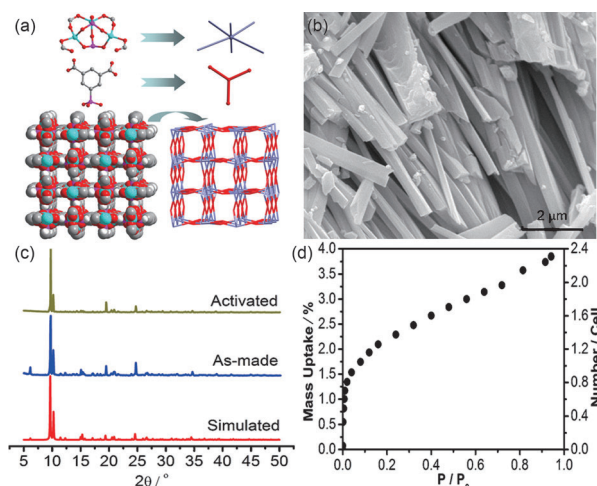


Figure 1. a) Crystal structure of ZnPC-2 constructed by a 6-connected trinuclear Zn^{II} cluster and 3-connected ligand. b) The SEM image of ZnPC-2 showing the rodlike structure of the crystals. c) The PXRD patterns of ZnPC-2 compared with that of simulated one. d) The adsorption amounts of toluene on activated ZnPC-2 at 298 K.

(CO_2)₄(PO_3)₂, $\text{Zn}_3\text{-SBU}$) and pbdc linkers (Figure 1a). The three Zn^{II} ions in the $\text{Zn}_3\text{-SBU}$ form an isosceles triangle with $\text{Zn}(1) \cdots \text{Zn}(1)^i$ ($i: x, 1/2-y, 1/4-z$) and $\text{Zn}(1) \cdots \text{Zn}(2)$ distances of 4.61 and 3.56 \AA , respectively. The oxygen atoms from the phosphonate of pbdc tridentately capture the isosceles triangle. Considering the $\text{Zn}_3\text{-SBU}$ as a 6-connected node formed with four C atoms from four carboxylates and two P atoms from two phosphonates as vertices and the pbdc as a 3-connected node, ZnPC-2 may be de-

scribed as a (3,6)-connected rutile-type network with approximately $6 \times 6 \text{ \AA}$ channels along the c axis and approximately $4 \times 4 \text{ \AA}$ along a and b axes by the taking van der Waals radius in consideration. SEM images of ZnPC-2 show the clear rodlike crystals with micrometer sizes (Figure 1b). PXRD patterns of the as-made and 110 °C activated samples are given in Figure 1c and both are well in agreement with the simulated data. No significant difference was observed from the different batch samples. Thermal stability of ZnPC-2 (see Figure S1 in the Supporting Information) was studied with TG analysis in the temperature range of 30–800 °C, showing a weight loss of about 5.0% from 30 to 150 °C ascribed to the loss of water molecules. To study the surface area and pore size of ZnPC-2, N_2 and Ar adsorption at 77 K were carried out, but no adsorption datum was obtained. The single-component vapor-phase adsorption of water, methanol and toluene were carried out on an automatic gravimetric adsorption apparatus at 298 K (see Figure S2 in the Supporting Information and Figure 1d). The adsorption curves of both methanol and water show a two-step weight increase (methanol at $P/P_0=0.2$ and water at $P/P_0=0.7$), which can be ascribed to the further uptake of guest molecules in the small channels of ZnPC-2 along the a and b axes. The adsorption behaviour of toluene on ZnPC-2 shows a type-I curve. The uptake amount increases rapidly and reaches 1.5 wt% (ca. 0.9 toluene/cell) at 0.04 P/P_0 , then increases linearly and reaches 3.8 wt% at P/P_0 of 0.94 ($P_0=3700 \text{ Pa}$ at 298 K), which may be ascribed to the further condensation of toluene on ZnPC-2. Thus, the analysis results show that the pure ZnPC-2 phase is obtained by the improved preparation method and the pore size of the product is enough to be accessed by toluene.

The isoreticular Hpd@ZnPC-2^[42] crystals were synthesized through a similar procedure as that of ZnPC-2, except by replacing triethylamine by pyrrolidine. The protonated pyrrolidine guests, based on single-crystal X-ray diffraction results (Figure 2), replace the hydrated protons of ZnPC-2, blocking the small channels along the a and b axes, but serving as walls of the large channels along the c axis. Because of the

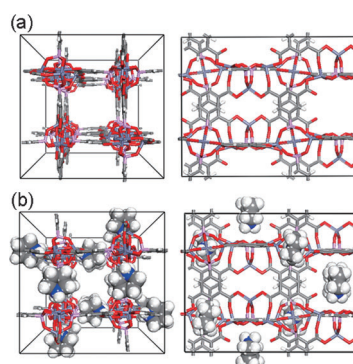
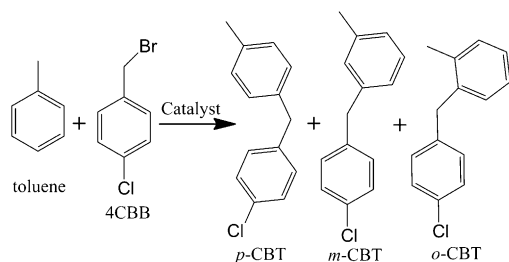


Figure 2. a) Perspective view of ZnPC-2 along the c axis (left) and orthographic view of ZnPC-2 along the b axis (right). b) The perspective view of Hpd@ZnPC-2 along the c axis showing the shrunken pore size (left) and orthographic view of Hpd@ZnPC-2 along the a axis (right) showing the position of Hpd (water molecules are omitted for clarity).

bulkier Hpd guests, the pore size of channels along the *c* axis is approximately 5×5 Å. The PXRD pattern (see Figure S3 in the Supporting Information) shows the product is pure. To identify the thermal stability of Hpd guest molecules in the framework, TGMS analysis results (see Figure S4 in the Supporting Information) show that the amine molecules are stable in the framework till 300 °C. Pyrrolidine molecules were detected after further increasing the temperature due to the collapse of the framework. Compared with the low thermal stability of amine-modified MOFs through the cation-exchange procedure,^[43] the high thermal stability of the amine guests in the ZnPC-2 framework may be ascribed to the strong hydrogen-bond interaction between the guest molecule and the host framework in restricted small channels along the *a* and *b* axes (see Figure S5 in the Supporting Information).

The CoZnPC-2 crystal sample was prepared by following a similar procedure with additional $\text{Co}(\text{OAc})_2 \cdot 4\text{H}_2\text{O}$ as the cobalt source described in the Experimental Section. The molar ratio of Zn/Co was varied from 8:1 to 1:2. Blue crystals of CoZnPC-2 were obtained when the ratio was set to 2:1 and the pure bulk sample was confirmed by PXRD patterns. Lowering or increasing the molar ratio will lead to the formation of other compounds besides CoZnPC-2 (see Figure S6 in the Supporting Information). Single-crystal X-ray diffraction (see Figures S7a and S7b and Table S1 in the Supporting Information) studies reveal that CoZnPC-2 is still a 3D rutile-type framework constructed of 6-connected trinuclear metal clusters and 3-connected pbdc ligands with the same coordination geometry. It has the *Fdd2* space group, which is different from that of ZnPC-2 and Hpd@ZnPC-2 in the *I-42d* space group. EDS analysis shows that the ratio of Zn/Co is about 1:1 in the product (see Figure S7c and S7d in the Supporting Information). Taking the single-crystal X-ray diffraction results into consideration, the Co^{II} and Zn^{II} ions are metal-atom disordered in the trinuclear metal cluster. The hydrated protons in CoZnPC-2 are filled in the large channels.

Catalytic reaction of ZnPC-2: The catalytic activity of ZnPC-2 was assessed by studying the Friedel–Crafts benzylation reaction of toluene with 4-chlorobenzyl bromide (4CBB) to form isochlorobenzyltoluene (CBT) products under ambient conditions (Scheme 1). The initial reaction was carried out by using 3 mol % ZnPC-2 catalyst relative to



Scheme 1. Friedel–Crafts benzylation reaction investigated by using ZnPC-2 as the catalyst.

4CBB at a certain temperature and the molar ratio of toluene to 4CBB was fixed to 50:1. The traditional Lewis acid catalyst of ZnCl_2 was used as a reference. The reaction mixture was analyzed at certain intervals by gas chromatography with nonane as a reference.

Effects of reaction temperature on the conversion of 4CBB were firstly studied in the range of 70–110 °C. As shown in Figure 3, the reaction at 70 °C reached a conver-

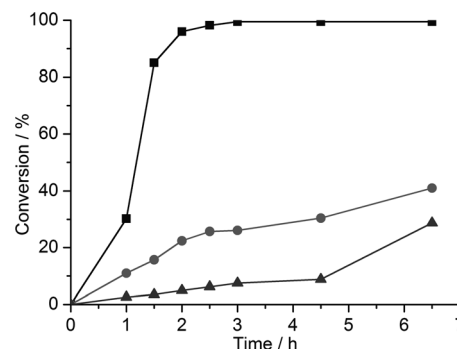


Figure 3. Catalytic performance of ZnPC-2 at 70, 90, and 110 °C. ■: 110 °C, ●: 90 °C, ▲: 70 °C.

sion of 29% after 6.5 h, and a longer reaction time (18 h) was required to achieve much higher conversion (78%). With increasing the temperature to 90 °C, the conversion boosted to be 41% after 6.5 h. At 110 °C, the >99% conversion of 4CBB was achieved within only 3 h, whereas the conversion was only 81% for ZnCl_2 . The high catalytic activity of ZnPC-2 is comparable to that of MOF-5.^[6] After the catalytic reaction, ZnPC-2 was centrifugally separated, and the PXRD pattern confirms its framework integrity after the reaction (see Figure S8 in the Supporting Information).

To prove whether or not the reaction occurs heterogeneously, the reaction solution was centrifugally separated from the catalyst after a one hour reaction time at 110 °C, transferred to a new vessel and then stirred for an additional 4 h at 110 °C. The GC result shows that there is no further conversion of 4CBB (see Figure S9 in the Supporting Information), which suggests that there is no contribution from leached active species,^[34] confirming the catalytic reaction is a heterogeneous process.

High catalytic selectivity is one of the crucial performances for catalysts. The selectivity of Friedel–Crafts benzylation reactions with traditional solid Lewis acidic catalysts, such as AlCl_3 , ZnCl_2 etc., is unsatisfactory. Therefore, the porous acidic catalysts with shape selectivity are highly desirable. In previous reports of MOF-5, the selectivity towards *para*-oriented products varied from 65 to 85% (dependent on reactants),^[6,34] which is higher than that of traditional Lewis catalysts. In our case, ZnPC-2 exhibits a high selectivity (>90%) for the less bulky *p*-CBT (Table 1), whereas ZnCl_2 is only about 54%, which is similar to previous reports.^[34] Generally, the high selectivity towards the

Table 1. Selectivity of the products of the Friedel–Crafts benzylation reaction of toluene with 4CBB (ZnPC-2 compared with the reference catalyst of ZnCl₂).

Catalyst	Selectivity [%]		
	<i>p</i> -CBT	<i>m</i> -CBT	<i>o</i> -CBT
ZnPC-2	91.4	7.3	1.3
ZnCl ₂	53.1	39.1	7.8

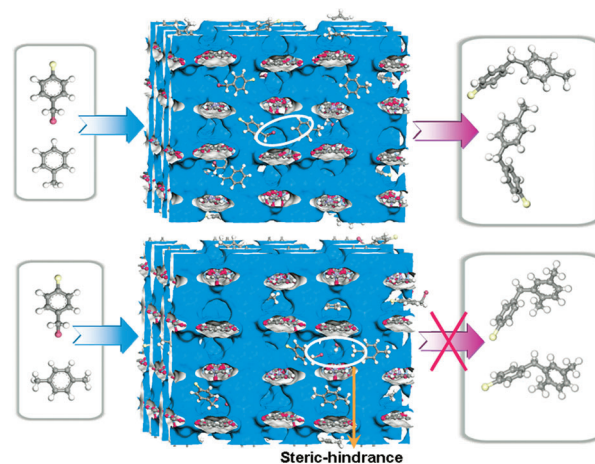
para-oriented product in porous MOFs is assumed to occur inside the pore, inhibiting the formation of large-size *meta*- and *ortho*- counterparts due to the steric-hindrance in restricted channels.^[6] However, direct evidence to prove this assumption has been rarely reported.

To investigate whether or not the catalytic reaction occurs inside the pore of ZnPC-2, benzylation reactions of toluene with different molecular sizes of 4CBB (11.3×4.3 Å, measured based on the ellipsoid structure), 3-biphenylmethylbromide (3BPMB, 12.7×5.7 Å) and 3,5-di-*tert*-butylbenzyl bromide (35TBBB, 10.4×7.3 Å) were carried out for 24 h. ZnCl₂ was still used as a reference catalyst with a conversion of >99% in all reactions involving 4CBB, 3BPMB and 35TBBB. ZnPC-2 exhibits a size-related selectivity towards these reactants to give a conversion of >99% for 4CBB, 89% for 3BPMB, and no conversion for 35TBBB. Based on these results, the selectivity of ZnPC-2 seems to be related to the regular channels along the *c* axis, which highly limits the diffusion of larger reactants and the formation of larger intermediates and products inside the pore. However, the external surface of ZnPC-2 also possibly contains active sites for 3BPMB. Therefore, an isoreticular framework with a shrunk pore size is necessary for further exploring the catalytic reaction.

Isoreticular frameworks with shrunk pore size can be prepared through two feasible approaches. One is to adjust the rigid organic linkers by the way similar to IRMOFs^[20] and the other is to post-modify the pore size with an organo reaction^[44] or guest exchange. However, it is a great challenge to obtain isoreticular frameworks based on phosphonate ligands because of its multidentate coordination nature. In our case, the isoreticular structure of Hpd@ZnPC-2 with the shrunk pore sizes was directly synthesized by using the pyrrolidine as the template. In Hpd@ZnPC-2, the Hpd guests block small channels along the *a* and *b* axes, and serve as the wall along the *c* axis. Because of its bulky size, the pore size is shrunk from approximately 6×6 Å in ZnPC-2 to approximately 5×5 Å in Hpd@ZnPC-2, which is smaller than the kinetic diameter of toluene (5.2 Å, size of the ellipsoid structure: ca. 4.6×5.7 Å). The Friedel–Crafts benzylation reaction of toluene with 4CBB over Hpd@ZnPC-2 shows an extremely low conversion of 4CBB (<1%) after 10 h, confirming that the catalytic reaction indeed occurs inside the pore of ZnPC-2.

Instead of toluene, *p*-xylene was further used to study whether or not the reaction occurs inside the pore of ZnPC-2. Generally, the Friedel–Crafts benzylation reactions of *p*-xylene with 4CBB form a pure product of 2-(4-chloroben-

zyl)-1,4-dimethylbenzene. Although the kinetic diameter of *p*-xylene (5.8 Å, size of the ellipsoid structure: ca. 4.6×6.9 Å) is smaller than the pore size of ZnPC-2, the size of the product, 2-(4-chlorobenzyl)-1,4-dimethylbenzene (size of its ellipsoid structure ca. 6.2×13.1 Å) is larger than the pore size of ZnPC-2. In addition, in a restricted space in ZnPC-2, the two methyl groups of *p*-xylene can be only placed parallel to the channel, which inhibits the Friedel–Crafts benzylation reaction of *p*-xylene with 4CBB due to the steric hindrance (Scheme 2). With the same reaction conditions as



Scheme 2. A snapshot of random uploading of guest molecules in a 2×2 cell of ZnPC-2 (top: the 4CBB and toluene; bottom: the 4CBB and *p*-xylene). A Drying force field was used to describe the interactions).

that of toluene, the catalytic result shows that there is no detectable conversion of 4CBB after 10 h, confirming that the benzylation reaction of toluene with 4CBB occurred inside the restricted channels of ZnPC-2, leading to the formation of the *para*-oriented product.

Understanding the active sites is very important for the design of high-performance heterogeneous catalysts. In the literature, the catalytic active sites of MOF-5 are ascribed to the structural defects,^[35] leading to the generation of Lewis acid sites. Recently, Co^{II}-substituted MOF-5 was reported for gas storage,^[45] which offers us a feasible method to explore the catalytic active sites of MOFs by metal-ion-substituted isoreticular frameworks. In our case, the catalytic active sites of ZnPC-2 are either related to the ligand or the Zn₃-SBU. With the same reaction conditions as those used for ZnPC-2, the Friedel–Crafts benzylation reaction was carried out by using the ligand as the catalyst. The result shows that there is no conversion of 4CBB after 10 h. Isoreticular frameworks of CoZnPC-2, in which part of Zn^{II} in Zn₃-SBU has been substituted by Co^{II} ions, was used as the catalyst. The results show that the conversion of 4CBB is near zero after 6 h, reaches 2% after 10 h and 7% after 18 h, which indicates that changing the constitution of Zn₃-SBU affects the catalytic performance. Taking the catalytic results of ligands and CoZnPC-2 into consideration, the immobilized

and regular distributed Zn₃-SBUs in ZnPC-2 are the catalytic active sites.

Conclusion

Three rutile-type porous zinc(II)-phosphonocarboxylate isoreticular frameworks of ZnPC-2, Hpd@ZnPC-2 and CoZnPC-2 have been successfully synthesized. In comparison with the conventional Lewis acid catalyst ZnCl₂, ZnPC-2 exhibits remarkable catalytic performance on the Friedel–Crafts benzylation reaction of toluene with 4-chlorobenzyl bromide, showing a high selectivity (>90%) to the *para* product because of its adaptable pore size. With the isoreticular frameworks of Hpd@ZnPC-2 and CoZnPC-2, it is proved that the catalytic reaction occurs inside the pore of ZnPC-2 and the catalytic active sites are the Zn₃-SBUs.

Experimental Section

Chemicals: All starting materials were obtained from commercial sources and used as received without any further purification unless otherwise noted. 4-Chlorobenzyl bromide was purchased from Acros and 3,5-di-*tert*-butylbenzyl bromide was purchased from TCI. Toluene and *p*-xylene were distilled before use. H₂pbdc was synthesized by the method described previously.^[41]

Synthesis of ZnPC-2, Hpd@ZnPC-2, and CoZnPC-2 catalysts: The layered-solvothermal synthesis method^[41] was used to obtain high quality crystals of {[Zn₃(pbdc)₂·2H₂O]_n} (ZnPC-2) and {[Zn₃(pbdc)₂·Hpd·H₃O·4H₂O]_n} (Hpd@ZnPC-2). In this work, an improved procedure was introduced for large-scale synthesis of the samples. For the synthesis of ZnPC-2, triethylamine (0.121 g, 1.21 mmol) was added to an isopropanol (5 mL) solution of H₂pbdc (0.075 g, 0.31 mmol). The white mixture was stirred until it became a clear solution. Then, the solution was added dropwise to another solution of Zn(CH₃COO)₂·2H₂O (0.101 g, 0.46 mmol) in deionized water (5 mL) for 10 min. After that the solution was stirred at room temperature for another 10 min and then transferred into a teflon-lined stainless steel autoclave (15 mL). After having been heated at 140 °C for 2 d, the autoclaves were cooled down to room temperature. The product of ZnPC-2 was collected by filtration (yield of 56% based on H₂pbdc). By replacing triethylamine by pyrrolidine, the product of Hpd@ZnPC was obtained (yield of 61% based on H₂pbdc).

CoZnPC-2 was synthesized by the following procedure: Zn(CH₃COO)₂·2H₂O (0.044 g, 0.20 mmol) and Co(CH₃COO)₂·4H₂O (0.025 g, 0.10 mmol) were dissolved in deionized water (5 mL) and heated at 50 °C for 30 min. The resulting pink solution was transferred to a teflon-lined stainless steel autoclave (15 mL) and then a solution of triethylamine (0.082 g, 0.82 mmol) and H₂pbdc (0.051 g, 0.21 mmol) dissolved in isopropanol (5 mL) was carefully layered above the pink solution. After the mixture had been sealed and heated at 140 °C for 3 d, the autoclaves were cooled down to room temperature. Yield is 24% based on H₂pbdc.

Crystallographic determination: Single-crystal CoZnPC-2 was mounted on a glass capillary and data collection was carried out on a Bruker Apex CCD diffractometer with graphite monochromated MoK_α radiation (λ = 0.71073 Å) at 293 K. Data reduction was performed with the SAINT and absorption corrections were applied by the SADABS program. The structure was solved by direct methods by using the SHELXS program and refined with SHELXL program. Heavy atoms and other non-hydrogen atoms are directly obtained from different Fourier maps. The disordered metal sites were then refined by using EXYZ and EADP methods. The final refinements were performed by the full-matrix least-square method

with anisotropic thermal parameters for all non-hydrogen atoms on F². Generally, C-bonded H atoms were placed geometrically and refined as riding modes, the hydrogen atoms of hydroprotons were not added due to their disordering. Crystallographic data including ZnPC-2, Hpd@ZnPC-2 and CoZnPC-2 are listed in Table S1 in the Supporting Information. CCDC-746203 (ZnPC-2), -776925 (Hpd@ZnPC-2) and -808302 (CoZnPC-2) contain the supplementary crystallographic data for this paper. These data can be obtained free of charge from The Cambridge Crystallographic Data Centre via www.ccdc.cam.ac.uk/data_request/cif.

Catalytic reactions: All the catalysts were degassed at 383 K for 3 h under 10⁻³ Pa before catalytic reactions. The Friedel–Crafts alkylation reactions were carried out under ambient conditions. In a typical reaction, a mixture of toluene (5 mL), 4-chlorobenzyl bromide (200.25 mg, 0.97 mmol) and nonane (0.2 mL) as an internal standard was added into a 50 mL flask containing the ZnPC-2 catalysts (17.50 mg, 0.024 mmol). The mixture was stirred at a desired temperature for a certain time. The products were analyzed by using gas chromatography at certain intervals and further confirmed by GCMS. The ZnPC-2 catalyst was separated from the reaction mixture by simple centrifugation, washed with anhydrous toluene, dried under vacuum at 383 K for 3 h and reused if necessary. An Agilent GC equipped with a flame-ionization detector (FID) and a DB-5 column was used for the reaction analyses by using nonane as an internal standard. The temperature program for GC analysis was settled as follows: held at 100 °C for 2 min., then heated from 100 to 250 °C at 20 °C min⁻¹ and held at this temperature for 10 min. Inlet and detector temperatures were set at 250 and 280 °C, respectively. The products were also identified by the ThermoFocus DSQ GC-MS chromatograph equipped with a FID and a HP-5 capillary column. MS results were compared with the data in the NIST library.

Characterization: Powder X-ray diffraction (PXRD) patterns were obtained on a Bruker D8 powder diffractometer by using a CuK_{α1} radiation (λ = 1.5405 Å) at 40 kV, 40 mA with a scan speed of 0.2 s/step and a step size of 0.02° (2θ). To identify the accessible pore size for toluene, the sorption isotherms were measured with an automatic gravimetric adsorption apparatus (IGA-001 series, Hiden Isochema Ltd.) at 298 K after samples were degassed at 383 K for 12 h. SEM images and EDS were obtained on a Philips XL-30 scanning electron microscope.

Acknowledgements

We gratefully acknowledge the NSF of China (nos. 21041009 and 91027044) and the Ministry of Sciences and Technology (no. 2009CB623506) for financial support.

- [1] C. Perego, S. Amarilli, A. Carati, C. Flego, G. Pazzuconi, C. Rizzo, G. Bellussi, *Microporous Mesoporous Mater.* **1999**, *27*, 345–354.
- [2] K. I. Shimizu, K. Niimi, A. Satsuma, *Appl. Catal. A* **2008**, *349*, 1–5.
- [3] G. A. Olah, *Friedel–Crafts Chemistry*, Wiley, New York, **1973**.
- [4] J. J. Chiu, D. J. Pine, S. T. Bishop, B. F. Chmelka, *J. Catal.* **2004**, *221*, 400–412.
- [5] K. Mantri, K. Komura, Y. Kubota, Y. Sugi, *J. Mol. Catal. A* **2005**, *236*, 168–175.
- [6] U. Ravon, M. E. Domine, C. Gaudillere, A. Desmartin-Chomel, D. Farrusseng, *New J. Chem.* **2008**, *32*, 937–940.
- [7] A. D. D. J. S. Beck, T. F. Degnan in *Zeolites for Cleaner Technologies. Catalytic Science Series, Vol. 3* (Eds.: M. Guisnet, J.-P. Gilson), Imperial College Press, London, **2002**, p. 223.
- [8] E. Armengol, M. L. Cano, A. Corma, H. Garcia, M. T. Navarro, *J. Chem. Soc. Chem. Commun.* **1995**, 519–520.
- [9] B. L. Chen, S. C. Xiang, G. D. Qian, *Acc. Chem. Res.* **2010**, *43*, 1115–1124.
- [10] T. Uemura, N. Yanai, S. Kitagawa, *Chem. Soc. Rev.* **2009**, *38*, 1228–1236.

- [11] L. J. Murray, M. Dinca, J. R. Long, *Chem. Soc. Rev.* **2009**, *38*, 1294–1314.
- [12] J. R. Li, R. J. Kuppler, H. C. Zhou, *Chem. Soc. Rev.* **2009**, *38*, 1477–1504.
- [13] A. U. Czaja, N. Trukhan, U. Muller, *Chem. Soc. Rev.* **2009**, *38*, 1284–1293.
- [14] S. Kitagawa, R. Matsuda, *Coord. Chem. Rev.* **2007**, *251*, 2490–2509.
- [15] H. X. Deng, C. J. Doonan, H. Furukawa, R. B. Ferreira, J. Towne, C. B. Knobler, B. Wang, O. M. Yaghi, *Science* **2010**, *327*, 846–850.
- [16] J. P. Zhang, X. C. Huang, X. M. Chen, *Chem. Soc. Rev.* **2009**, *38*, 2385–2396.
- [17] D. J. L. Tranchemontagne, Z. Ni, M. O’Keeffe, O. M. Yaghi, *Angew. Chem.* **2008**, *120*, 5214–5225; *Angew. Chem. Int. Ed.* **2008**, *47*, 5136–5147.
- [18] H. K. Chae, D. Y. Siberio-Perez, J. Kim, Y. Go, M. Eddaoudi, A. J. Matzger, M. O’Keeffe, O. M. Yaghi, *Nature* **2004**, *427*, 523–527.
- [19] O. M. Yaghi, M. O’Keeffe, N. W. Ockwig, H. K. Chae, M. Eddaoudi, J. Kim, *Nature* **2003**, *423*, 705–714.
- [20] M. Eddaoudi, J. Kim, N. Rosi, D. Vodak, J. Wachter, M. O’Keeffe, O. M. Yaghi, *Science* **2002**, *295*, 469–472.
- [21] X. Gu, Z. H. Lu, Q. Xu, *Chem. Commun.* **2010**, *46*, 7400–7402.
- [22] N. Klein, I. Senkovska, K. Gedrich, U. Stoeck, A. Henschel, U. Mueller, S. Kaskel, *Angew. Chem.* **2009**, *121*, 10139–10142; *Angew. Chem. Int. Ed.* **2009**, *48*, 9954–9957.
- [23] Q. R. Fang, G. S. Zhu, Z. Jin, Y. Y. Ji, J. W. Ye, M. Xue, H. Yang, Y. Wang, S. L. Qiu, *Angew. Chem.* **2007**, *119*, 6758–6762; *Angew. Chem. Int. Ed.* **2007**, *46*, 6638–6642.
- [24] X. S. Wang, S. Ma, D. Sun, S. Parkin, H. C. Zhou, *J. Am. Chem. Soc.* **2006**, *128*, 16474–16475.
- [25] R. Matsuda, R. Kitaura, S. Kitagawa, Y. Kubota, R. V. Belosludov, T. C. Kobayashi, H. Sakamoto, T. Chiba, M. Takata, Y. Kawazoe, Y. Mita, *Nature* **2005**, *436*, 238–241.
- [26] J. B. Lin, J. P. Zhang, X. M. Chen, *J. Am. Chem. Soc.* **2010**, *132*, 6654–6655.
- [27] D. M. Jiang, T. Mallat, D. M. Meier, A. Urakawa, A. Baiker, *J. Catal.* **2010**, *270*, 26–33.
- [28] J. Meeuwissen, J. N. H. Reek, *Nat. Chem.* **2010**, *2*, 615–621.
- [29] L. Pan, H. M. Liu, X. G. Lei, X. Y. Huang, D. H. Olson, N. J. Turro, J. Li, *Angew. Chem.* **2003**, *115*, 560–564; *Angew. Chem. Int. Ed.* **2003**, *42*, 542–543.
- [30] J. Lee, O. K. Farha, J. Roberts, K. A. Scheidt, S. T. Nguyen, J. T. Hupp, *Chem. Soc. Rev.* **2009**, *38*, 1450–1459.
- [31] D. Farrusseng, S. Aguado, C. Pinel, *Angew. Chem.* **2009**, *121*, 7638–7649; *Angew. Chem. Int. Ed.* **2009**, *48*, 7502–7513.
- [32] A. Corma, H. Garcia, F. X. L. Xamena, *Chem. Rev.* **2010**, *110*, 4606–4655.
- [33] Y. Liu, W. M. Xuan, Y. Cui, *Adv. Mater.* **2010**, *22*, 4112–4135.
- [34] N. T. S. Phan, K. K. A. Le, T. D. Phan, *Appl. Catal. A* **2010**, *382*, 246–253.
- [35] U. Ravon, M. Savonnet, S. Aguado, M. E. Domine, E. Janneau, D. Farrusseng, *Microporous Mesoporous Mater.* **2010**, *129*, 319–329.
- [36] C. A. Fernandez, P. K. Thallapally, J. Liu, C. H. F. Peden, *Cryst. Growth Des.* **2010**, *10*, 4118–4122.
- [37] P. Horcajada, S. Surble, C. Serre, D. Y. Hong, Y. K. Seo, J. S. Chang, J. M. Greneche, I. Margiolaki, G. Ferey, *Chem. Commun.* **2007**, 2820–2822.
- [38] N. W. Ockwig, O. Delgado-Friedrichs, M. O’Keeffe, O. M. Yaghi, *Acc. Chem. Res.* **2005**, *38*, 176–182.
- [39] L. Q. Ma, J. M. Falkowski, C. Abney, W. B. Lin, *Nat. Chem.* **2010**, *2*, 838–846.
- [40] F. J. Song, C. Wang, J. M. Falkowski, L. Q. Ma, W. B. Lin, *J. Am. Chem. Soc.* **2010**, *132*, 15390–15398.
- [41] T. B. Liao, Y. Ling, Z. X. Chen, Y. M. Zhou, L. H. Weng, *Chem. Commun.* **2010**, *46*, 1100–1102.
- [42] Y. Ling, T. B. Liao, Z. X. Chen, Y. M. Zhou, L. H. Weng, *Dalton Trans.* **2010**, *39*, 10712–10718.
- [43] J. An, N. L. Rosi, *J. Am. Chem. Soc.* **2010**, *132*, 5578–5579.
- [44] Z. Q. Wang, S. M. Cohen, *Chem. Soc. Rev.* **2009**, *38*, 1315–1329.
- [45] J. A. Botas, G. Calleja, M. Sanchez-Sanchez, M. G. Orcajo, *Langmuir* **2010**, *26*, 5300–5303.

Received: April 22, 2011
Published online: August 4, 2011